Comparing DMT Variants in Medium-Reach 100G Optically Amplified Systems

Comparing DMT Variants in Medium-Reach 100G Optically Amplified Systems

Dario Pilori, *Student Member, OSA*, Chris Fludger and Roberto Gaudino, *Senior Member, IEEE*

***Abstract*—Several research works are currently addressing 100+ Gbps per wavelength high-capacity DWDM medium reach systems (80 km on SMF fibers) to cover the metro market segment. For the purposes of cost reduction, it is interesting to consider the use of direct detection receivers rather than the more expensive coherent receivers. However, DWDM transmission in the C-Band imposes severe limitations in terms of tolerances to chromatic dispersion, electrical low-pass filtering, Analog-to-Digital Converter (ADC) and Digital-to-Analog Converter (DAC) quantization effects and receiver optical signal to noise ratio (OSNR). In this paper, we analyze the ultimate performance of several variances of Discrete Multitone (DMT) modulation (namely Dual-SideBand DMT, Single-SideBand and Vestigial-SideBand), comparing them in terms of required OSNR as a function of several system parameters in a medium reach scenario. We found that for the 80 km target link only single-sideband DMT seems a viable option, while double-sideband DMT has exceedingly high OSNR requirements.**

***Index Terms*—Digital Multitone (DMT) Modulation, medium-reach optical links, 100 Gbps per wavelength transmission.**

I. Introduction

OPTICAL transmission systems are steadily evolving to 100+ Gbps per wavelength solutions in several market segments, from the inter-data center to the long-haul systems. While in long-haul the clear winner is the combination of advanced modulation formats, Digital Signal Processing (DSP) and coherent detection, the situation is less clear for shorter links, so that several recent research papers have addressed solutions that retain less-expensive direct detection receivers coupling them with advanced modulation formats and DSP [1]–[4]. Our research focuses on 100+ Gbps on a "medium-reach" scenario characterized by distances up to 80 km, using optical pre-amplification in front of direct detection receiver and operating in the C-Band in order to be compliant with Dense Wavelength Division Multiplexing (DWDM). This scenario is typically applicable to next-generation ultra-high capacity metro network. If one wants to target 100 Gbps (or more) per λ over these links, traditional On-Off Keying (OOK) is completely out of question, due to electrical bandwidth limitations and the exceedingly strong impact of chromatic dispersion, which cannot be reasonably counteracted by any form of electronic equalization at the receiver. Additionally, PAM-4 solutions currently under standardization for 100 Gbps solutions over short link (*i.e.* up to 2 km) seems also very sensitive in the previously described medium-reach scenario, particularly due to chromatic dispersion (unless *optical* chromatic dispersion compensation is used, an option that is intentionally neglected in this paper).

One of the solutions that have been investigated by several groups to allow 100 Gbps per λ in this medium-haul scenario is using several variants of Discrete Multitone (DMT) [2], [5], [6].

In this paper, we focus on a detailed comparison of the transmission performance in the previously described medium reach scenario for three DMT variants, carried out through a combination of theoretical assessment and numerical simulations. Our main goal is to establish the ultimate performance in terms of required Optical Signal-to-Noise Ratio (OSNR) at the receiver and highlight the different types of system penalties. The three DMT variants that we analyze are:

- Dual Side-Band (DSB) DMT, in which the instantaneous power of the transmitted optical signal is power-modulated by a positive and real-valued DMT signal. The resulting optical spectrum is double-sided and requires a total bandwidth that is twice the bandwidth of the real DMT signal.
- Single Side-Band (SSB) DMT, in which the transmitted electrical field is modulated in such a way that one of the two optical sidebands is removed but the signal can still be directly-detected due to a self-coherent effect made possible by the presence of a sufficiently strong unmodulated optical carrier.
- Vestigial Side-Band (VSB) DMT which is a hybrid of the previous two cases in which a DSB-DMT signal is optically filtered to remove one of the two sidebands.

The novelty of this paper is in the joint assessment of the three modulations addressing the different sources of OSNR penalty. To this end, the paper is organized as follows. In Sec.II we start by evaluating the OSNR requirements assuming ideally spectrally flat electrical and optical components for the three modulation formats. We use in this Section a mix of analytic formulas and numerical simulations, in order to derive the receiver sensitivity in terms of OSNR requirement for an ideal optical back-to-back scenario. In the following Sec.III we analyze the chromatic dispersion penalty and the need for bit and power loading algorithms. Finally, in Sec.IV, we introduce realistic bandwidth limitations for the most critical electrical components and the very relevant impact of the finite resolution of ADC and DAC.

D. Pilori and R. Gaudino are with Department of Electronics and Telecommunications (DET), Politecnico di Torino, Italy. E-Mail: dario.pilori@polito.it, roberto.gaudino@polito.it.

C. Fludger is with Cisco Optical GmbH, Nuremberg 90411, Germany. E-Mail: cfludger@cisco.com

In all three Sections II-IV we also discuss the need for DSP-based compensation of some unwanted quadratic terms, a well-known issue for SSB-DMT [1], [5], [7]. One of the new results of this paper is in pointing out that nonlinear (quadratic) compensation can also be highly beneficial for DSB and SSB, where we propose new and relatively simple DSP algorithms.

The main outcome of this paper can be summarized as follows: for the 100 Gbps per wavelength target, DSB-DMT has almost the same OSNR performance as SSB-DMT for relatively short systems (below 10 km) and thus it seems the most promising candidate among the three different options, since it has lower complexity in terms of both optical components requirements and DSP. Anyway, for the target 80 km SMF and C-band (1550 nm) scenario, DSB-DMT has an unacceptably high penalty due to chromatic dispersion, while SSB-DMT is very promising since it has low penalty compared to the back-to-back scenario even at the expense of an increase in complexity of both optoelectronics and DSP. The VSB-DMT solution is a compromise between the two options. We also found that the "power-modulated" DSB and VSB options have a very strong requirements in terms of DAC and ADC resolution (i.e in terms of Effective Number of Bits or ENoB parameter), while SSB is less sensitive to this issue.

II. Back-to-Back Performances

A. Methodology

In this Section, the performance of DSB, SSB and VSB DMT is evaluated in optical back-to-back, with the aim of assessing the minimum required OSNR for each modulation format when assuming ideal components and in particular spectrally flat ADCs, DACs, modulators and photodiodes, and no quantization effects in ADCs and DACs. The transmitted block diagrams and the resulting qualitative spectrum for the three cases are shown in Fig.1.

In this Section, $x(t)$ is an ideal real-valued DMT signal generated by a Digital Signal Processing (DSP) running at R_s samples/s and thus creating a flat signal spectrum in the bandwidth between $-R_s/2$ and $R_s/2$ (and zero outside it). When relevant for the analytic derivation, the DMT signal $x(t)$ is assumed to be a Gaussian random process with zero mean and variance (power) σ_x^2.

The performance of these methods has been evaluated using either analytic expressions or time-domain numerical simulations. In the numerical examples of this Section, $x(t)$ is a 16-QAM DMT signal with $R_s = 64$ Gs/s, which is a typical value for today's top-class ADCs and DACs. For these simulations, DAC and ADC are assumed to be completely ideal (flat frequency response inside the bandwidth, no quantization). FFT size is 512, and the number of modulated subcarriers is 255.

Considering that each subcarrier carries $n_{bit} = 4$ information bits, the resulting gross bit rate is $R_s/2 \cdot n_{bit} = 128$ Gbit/s, a value that we select since it should be able to support 100 Gbps net including the required overhead. The optical channel adds only Amplified Spontaneous Emission (ASE) noise, and the resulting OSNR is calculated over a bandwidth $B_o = 0.1$ nm.

As a performance metric, the receiver evaluates the Signal-to-Noise Ratio (SNR) E_s/N_0 for each DMT subcarrier by comparing the received noisy constellations with the ideal transmitted ones. Afterwards, the receiver calculates the geometric mean over all subcarriers that, as explained in details in [8], is the single-channel equivalent SNR for DMT systems.

B. Dual Side-Band

1) Modulation: For DSB DMT, the optical signal is assumed to be modulated using a power modulator (*e.g.* a directly modulated laser but with negligible chirp) as shown in Fig.1, therefore the optical field at the output of the modulator can be written using the complex envelope notation as:

$$E_{TX}^{(dsb)}(t) = \sqrt{P_{out}(t)} = \sqrt{\bar{P}\left\{1 + \mathcal{Q}\left[\frac{x(t)}{c'}\right]\right\}} \quad (1)$$

$P_{out}(t)$ is the instantaneous output optical power, $\bar{P}$ is the average transmit optical power, and $\mathcal{Q}$ is a clipping function (*i.e.* a symmetrical hard limiter) that forces the transmitted power to be positive, defined as:

$$\mathcal{Q}(\alpha) = \begin{cases} \alpha & -1 \le \alpha \le 1 \\ -1 & \alpha < -1 \\ 1 & \alpha > 1 \end{cases} \quad (2)$$

The parameter c' in the previous equation allows to set a specific *clipping ratio*, defined as the ratio between the clipping threshold squared and the power of input signal [6]

$$R_{cl} = \frac{c'^2}{\sigma_x^2} \quad (3)$$

The previous notation means that the DMT signal $x(t)$ is hard-limited between $\pm\sqrt{R_{cl} \cdot \sigma_x^2}$. The clipping ratio is a very important parameter for DSB, as explained in several previous papers such as [6] since a small R_{cl} clipping ratio will add high clipping noise, while a large clipping ratio will decrease the power of the useful signal in (1) thus reducing the effective tolerance to noise. As it will be shown later, the clipping ratio has a strong impact on system performance.

2) Clipping ratio and CSPR: It is useful to introduce the Carrier to Signal Power Ratio (CSPR) on the modulated optical signal, since it allows a comparison with other DMT techniques. The Carrier-to-Signal Power Ratio (CSPR) ξ is defined here as the ratio between the optical power of the un-modulated Continuous Wave (CW) carrier transmitted (see previous qualitative spectrum in Fig.1) and the power of the modulated signal or, in formula:

$$\xi^{(dsb)} = \frac{\mathbb{E}^2\left\{E_{TX}^{(dsb)}(t)\right\}}{\mathrm{var}\left\{E_{TX}^{(dsb)}(t)\right\}} \quad (4)$$

where $\mathbb{E}$ denotes expectation and var variance. It turns out that the CSPR for DSB-DMT depends only on the clipping ratio. Assuming $\xi^{(dsb)} \gg 1$ (as it is always the case, see later), (1) can be expanded using a Taylor's series expansion, obtaining

$$E_{TX}^{(dsb)}(t) \approx \sqrt{\bar{P}}\left[1 + \frac{y(t)}{2} - \frac{y^2(t)}{8} + \frac{y^3(t)}{16} - \frac{5y^4(t)}{128}\right] \quad (5)$$

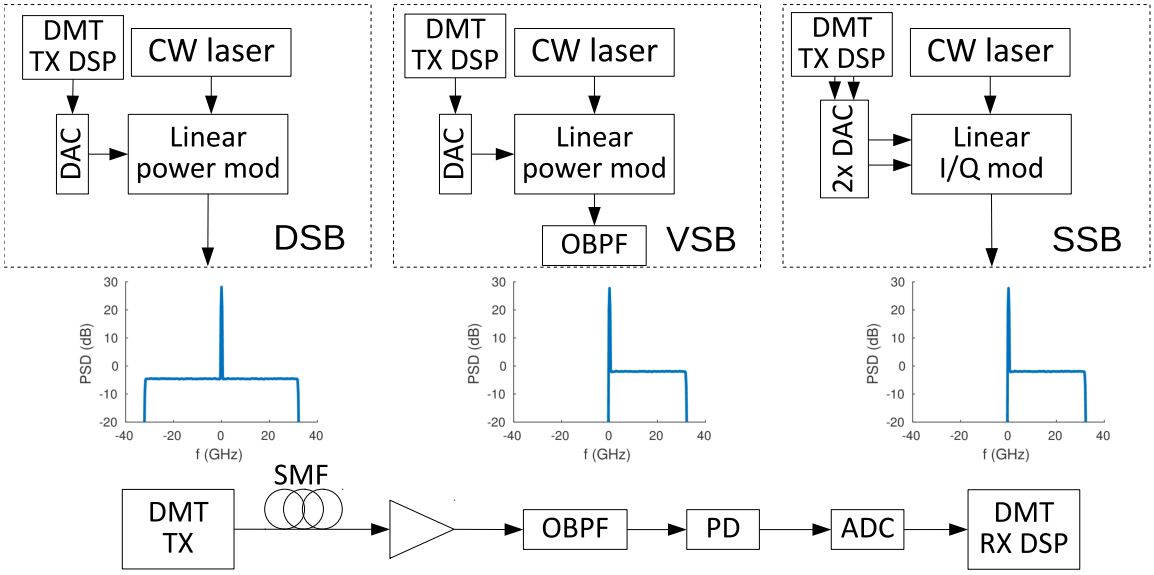

Fig. 1. Transmitter block diagram and qualitative spectrum of the three DMT variants addressed in this paper.

where $y(t)$ is defined as

$$y(t) = \mathcal{Q}\left[\frac{x(t)}{c'}\right] \tag{6}$$

Since in all situations of interest $\xi^{(\mathrm{dsb})} \gg 1$ (as we will show later), $y(t)$ can still be approximated as a Gaussian random process, with zero mean and variance σ_{y}^2. Substituting (5) into (4), the CSPR can be approximated as

$$\xi^{(\mathrm{dsb})} \approx \frac{\left(1 - \frac{1}{8}\sigma_{\mathrm{y}}^2 - \frac{15}{128}\sigma_{\mathrm{y}}^4\right)^2}{1 - \left(1 - \frac{1}{8}\sigma_{\mathrm{y}}^2 - \frac{15}{128}\sigma_{\mathrm{y}}^4\right)^2} \tag{7}$$

This equation can be solved numerically to obtain the variance of y needed to achieve a specific CSPR, and from this the required clipping ratio.

If clipping effects can be neglected, *i.e.* for high values of R_{cl}, the variance of y is inversely proportional to the clipping ratio

$$\sigma_{\mathrm{y}}^2 \approx \frac{\sigma_{\mathrm{x}}^2}{c'^2} = \frac{1}{R_{\mathrm{cl}}} \tag{8}$$

which in turn allows a direct relation between the clipping ratio and the CSPR as shown in Fig.2. The solid blue line is a numerical evaluation of (4), while the dashed line is the approximation obtained using (7) (8). In the range of interest of clipping ratio (typically well above 8-9 dB, as shown later), the approximation is quite accurate, with a maximum error lower than 0.5 dB. In fact, for high values of CSPR, which also mean high clipping parameter (*i.e.* small clipping on the useful signal), (7) be further simplified by only considering lower order terms in the Taylor series expansion in (5)

$$\xi^{(\mathrm{dsb})} \approx 4R_{\mathrm{cl}} \tag{9}$$

In conclusion, we observe that asymptotically the relation between these two parameters is linear, and in particular $\mathrm{CSPR}_{\mathrm{dB}} \approx R_{\mathrm{cl,dB}} + 6$ dB. From a system point of view, the price to be paid in DSB-DMT to minimize clipping effects is to keep a strong un-modulated CW carrier on the transmitted optical field.

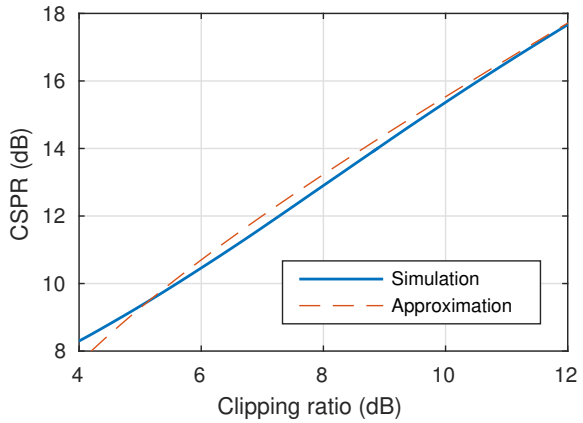

Fig. 2. Relation between clipping ratio and CSPR. Solid line: numerical evaluation of (4), dashed line: approximation of (7) neglecting clipping.

3) Performance with received optical noise: Assuming an ideal (optical and electrical) channel, *i.e.* without any bandwidth limitation or distortion, the received electric field is the transmitted electric field with the addition of complex-valued ASE noise in both polarizations ($n_{\mathrm{X}}(t)$ and $n_{\mathrm{Y}}(t)$), given by:

$$E_{\mathrm{RX}}^{(\mathrm{dsb})}(t) = \left[E_{\mathrm{TX}}^{(\mathrm{dsb})}(t) + n_{\mathrm{X}}(t)\right]\hat{\mathbf{i}}_{\mathrm{X}} + n_{\mathrm{Y}}(t)\hat{\mathbf{i}}_{\mathrm{Y}} \tag{10}$$

where $\hat{\mathbf{i}}_{\mathrm{X}}$ and $\hat{\mathbf{i}}_{\mathrm{Y}}$ are unit vectors in polarization space. The power of noise in both polarizations over an integration bandwidth B_{o} (*e.g.* 0.1 nm) is $2N_0B_{\mathrm{o}}$, which can be expressed in terms of OSNR:

$$\mathrm{OSNR} = \frac{\bar{P}}{2N_0B_{\mathrm{o}}} \tag{11}$$

4) Direct detection: After direct detection with an ideal photodiode, neglecting irrelevant conversion constants, the

electrical signal can be expressed as:

$$z^{(\mathrm{dsb})}(t) = \left|E_{\mathrm{RX}}^{(\mathrm{dsb})}(t)\right|^2 = \bar{P} + \bar{P}\,\mathcal{Q}\left[\frac{x(t)}{c'}\right] + |n_{\mathrm{X}}(t)|^2 + \\ + |n_{\mathrm{Y}}(t)|^2 + 2n_{\mathrm{X,I}}(t)\sqrt{\bar{P}\left\{1+\mathcal{Q}\left[\frac{x(t)}{c'}\right]\right\}} \quad (12)$$

where $n_{\mathrm{X,I}}(t) = \Re\{n_{\mathrm{X}}(t)\}$. Assuming OSNR $\gg 1$, the noise-noise beating terms can be neglected (an assumption that will be verified a posteriori in the following section) leading to the following simplified received signal:

$$z_0^{(\mathrm{dsb})}(t) \approx \bar{P}\,\mathcal{Q}\left[\frac{x(t)}{c'}\right] + 2n_{\mathrm{X,I}}(t)\sqrt{\bar{P}\left\{1+\mathcal{Q}\left[\frac{x(t)}{c'}\right]\right\}} \quad (13)$$

where the pedix $_0$ denotes removal of the irrelevant DC component.

After sampling (13) with rate R_{s}, the powers of signal and noise can be evaluated in order to calculate the electrical SNR. Neglecting the effect of clipping, the power of the signal can be approximated as

$$P_{\mathrm{s}} \approx \frac{\bar{P}^2\sigma_{\mathrm{x}}^2}{c'^2} = \frac{\bar{P}^2}{R_{\mathrm{cl}}} \quad (14)$$

while the power of noise, assuming that is uncorrelated with the signal, is

$$P_{\mathrm{n}} = 2N_0R_{\mathrm{s}}\bar{P} \quad (15)$$

This leads to a simple expression that approximates the relation between the electrical SNR, the OSNR defined in (11) and the clipping ratio

$$E_{\mathrm{s}}/N_0 = \frac{\bar{P}}{R_{\mathrm{cl}}R_{\mathrm{s}}2N_0} = \frac{\mathrm{OSNR}}{R_{\mathrm{cl}}}\cdot\frac{B_{\mathrm{o}}}{R_{\mathrm{s}}} \quad (16)$$

Using the approximation in (9), it can also be related to the CSPR $\xi^{(\mathrm{dsb})}$

$$E_{\mathrm{s}}/N_0 \approx \mathrm{OSNR}\cdot\frac{4B_{\mathrm{o}}}{R_{\mathrm{s}}}\cdot\frac{1}{\xi^{(\mathrm{dsb})}} \quad (17)$$

Regarding noise-noise beating, which was neglected in (13), its power is

$$P_{\text{nois-nois}} = (2N_0R_{\mathrm{s}})^2 \quad (18)$$

Comparing this equation with (15), its power is lower than signal-noise beating by a factor of OSNR $\cdot\, B_{\mathrm{o}}/R_{\mathrm{s}}$. For the values of interest of OSNR, this term is large, and the impact of noise-noise beating in the electrical SNR (17) is below 0.03 dB in all the considered cases.

This last equation has a very important system interpretation: the electrical SNR is inversely proportional to the CSPR (or equivalently to the clipping ratio in the asymptotic approximation), therefore for instance an increase by 1 dB in CSPR will decrease by 1 dB the electrical SNR at the receiver. This can be very simply understood: increasing the CSPR by 1 dB means adding 1 dB to the unmodulated optical carrier, which is "useless" for the actual detection of data in noise, at the expenses of the power of the modulated part of the spectrum.

Fig.3 reports the electrical SNR in a 16-QAM DMT simulation as a function of the CSPR, where the red dashed line is

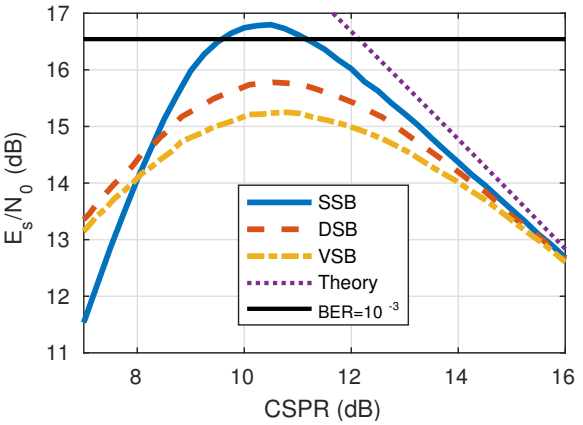

Fig. 3. Comparison of 16-QAM DMT SSB (blue solid line), DSB (red dashed line) and VSB (yellow dash-dot line) with an OSNR=30 dB over 0.1 nm. Results are compared with the theoretical asymptotical SNR (purple dot line) (17), and the minimum SNR required to obtain a BER=10^{-3} (black solid line).

for the DSB case while the other curves will be introduced in the following sections. The simulation results are compared with the asymptotic approximation in (17) (dotted purple line). As illustrated in the Figure, the electrical SNR peaks at $\xi^{(\mathrm{dsb})} = 10.5$ dB. For high values of CSPR the curve gets closer to the approximation (17), since clipping noise becomes negligible and the approximations performed in the previous equations become more accurate. On the other end, for low values of CSPR, the SNR decreases due to clipping noise, which is not taken into account in (17). In conclusion, for the ideally spectrally flat conditions assumed in this Section, the DSB optimal operating point is a careful balance between clipping noise and loss of modulated signal power, as denoted by CSPR.

C. Single Side-Band

1) Modulation: To generate a SSB-DMT signal, it is necessary to use a field modulator (*e.g.* dual-nested Mach-Zehnder modulator in its linear region) as shown in Fig.1. In order to obtain the Single Side-Band spectrum, the optical field at the output of the modulator must be given by:

$$E_{\mathrm{TX}}^{(\mathrm{ssb})}(t) = \frac{1}{\sqrt{2}}\left[x(t) + j\,\mathcal{H}\{x(t)\}\right] + c \quad (19)$$

where c is the CW carrier amplitude, and $\mathcal{H}\{\cdot\}$ indicates Hilbert transform, defined as the convolution with a linear filter with frequency response

$$H_{\mathrm{hilb}}(f) = \begin{cases} j & f > 0 \\ 0 & f = 0 \\ -j & f < 0 \end{cases} \quad (20)$$

The addition of the Hilbert transform on the imaginary component eliminates the negative frequency components of $E_{\mathrm{TX}}^{(\mathrm{ssb})}(t)$, thus creating an SSB signal. Multiplication by $1/\sqrt{2}$ is introduced so that the power of the modulated part of the signal is the same as $x(t)$.

The need to add a carrier c to the signal is necessary to allow direct detection with a photodiode, but it once again leads to a transmit electric field with CSPR:

$$\xi^{(\mathrm{ssb})} = \frac{c^2}{\sigma_{\mathrm{x}}^2} \tag{21}$$

In contrast to DSB, the CSPR in SSB is not related to signal clipping, but it is a parameter that can be freely chosen at the modulator changing c or σ_{x}^2. The independence between CSPR and signal clipping gives a significant system advantage of SSB over DSB, as shown later.

2) Direct detection for SSB: After the addition of ASE noise (10), the signal is first filtered with an ideal Optical Band-Pass Filter (OBPF) with bandwidth $R_{\mathrm{s}}/2$, and then it is detected with an ideal photodiode (see again Fig.1). Applying the same approximations used for DSB, *i.e.* neglecting noise-noise beating, noise-signal beating and removing DC, the received signal after the photodiode is

$$z_0^{(\mathrm{ssb})}(t) \approx \frac{1}{2}\left[x^2(t) + \mathcal{H}^2\{x(t)\}\right] + 2c\left[\frac{1}{\sqrt{2}}x(t) + n_{\mathrm{X,I}}(t)\right] \tag{22}$$

Comparing this equation with DSB (13), it is evident that there is an additional self-interference term given by:

$$x_{\mathrm{SSBI}}(t) = \frac{1}{2}\left[x^2(t) + \mathcal{H}^2\{x(t)\}\right] \tag{23}$$

This term is called Signal-Signal Beating Interference (SSBI) and, if not compensated, represents a penalty for the receiver.

It was experimentally shown [1], [5], [7], [9], [10] that SSBI can be almost completely removed by proper algorithms in the receiver DSP, with an effectiveness that depends also on the CSPR value. Under the simplifying assumption of SSBI perfect cancellation, the electrical SNR can be easily calculated from (22) as:

$$E_{\mathrm{s}}/N_0 = \frac{2\sigma_{\mathrm{x}}^2}{R_{\mathrm{s}}N_0} = \mathrm{OSNR}\frac{4B_{\mathrm{o}}}{R_{\mathrm{s}}\left(1+\xi^{(\mathrm{ssb})}\right)} \tag{24}$$

This equation is similar to the approximation for DSB in (16).

For high values of CSPR, (16) can be approximated as (17), and neglecting $+1$ in the denominator of (24) the two results become equal. From a system point of view this means that for sufficiently high CSPR, DSB-DMT has asymptotically the same performance of SSBI-cancelled SSB-DMT, even if the DSB signal occupies twice the optical bandwidth compared to SSB. This effect can be understood by comparing the signals after photodetection for DSB (13) and SSB (22). While noise power is doubled in DSB compared to SSB, since it is sampled over twice the bandwidth, signal power is also doubled, due to the combination of the two sidebands (which contain the same information).

In conclusion, in the ideal optical back-to-back case studied in this section DSB and SSB DMT have the same asymptotical performance for high CSPR but the actual DSB-DMT is limited by clipping effects, while SSB-DMT can be limited by the quality of the SSBI cancellation algorithm, as discussed in the following Subsection.

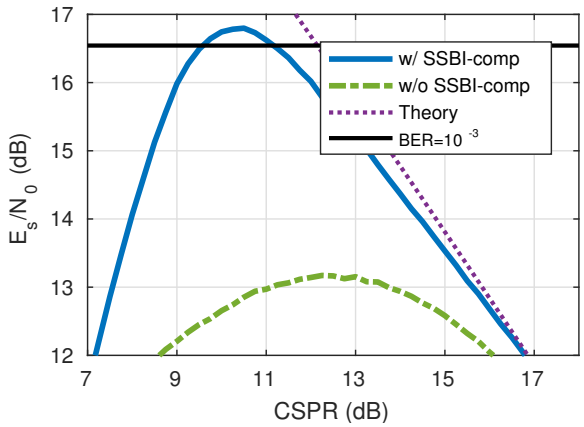

Fig. 4. SNR, geometrically averaged over all the subcarriers, of a SSB-DMT signal, with (solid blue line) and without (green dash-dot line) SSBI compensation. The OSNR is 30 dB over 0.1 nm, $R_{\mathrm{s}} = 64$ Gs/s, constellation is 16-QAM on all subcarriers. Results are compared with the minimum SNR required to obtain BER=10^{-3} (black solid line).

3) SSBI compensation: There are several techniques shown in literature to compensate SSBI [1], [5], [7], [9]. For this work, we adopted the method described in [1], which represents a good compromise between effectiveness and computational complexity. This scheme estimates SSBI at the receiver as

$$\hat{x}_{\mathrm{SSBI}}(t) = \gamma\left|z_0^{(\mathrm{ssb})}(t) + j\,\mathcal{H}\left\{z_0^{(\mathrm{ssb})}(t)\right\}\right|^2 \tag{25}$$

where γ is a positive real-valued coefficient, optimized at the receiver, and $z_0^{(\mathrm{ssb})}(t)$ is the received signal after the photodiode.

Fig.4 compares the SNR E_{s}/N_0 of a 16-QAM SSB-DMT signal, with and without SSBI compensation. The compensation scheme is able to increases the SNR by ~ 3.5 dB at the optimal CSPR. The SSBI compensated system has an SNR which is very similar to the theoretical asymptotic value for sufficiently large CSPR values, while for smaller CSPR the estimation error becomes too large, strongly decreasing the electrical SNR.

A comparison between SSB with SSBI compensation (blue solid line) and DSB is shown in Fig.3, which is one of the main results of the first part of this paper. It is noteworthy that the shape of the two curves is similar, showing a maximum SNR for approximately the same CSPR value (about 10.5 dB). At this optimal CSPR value, SSB has a 1.4 dB advantage over DSB. For smaller values of CSPR, DSB is limited by clipping effects while SSB is limited by imperfect SSBI cancellation. In contrast, SSB transmission without SSBI cancellation is significantly worse than that of DSB.

D. Vestigial Side-Band

1) Modulation: A Vestigial Side-Band signal is here defined as a DSB-DMT that is optically filtered at the transmitter in order to (at least partially) suppress one sideband, as shown in Fig.1. This approach potentially allows the generation of a signal similar to SSB with a smaller transmitter complexity.

Assuming here an ideal rectangular optical filter that cuts one of the two sidebands, the VSB transmit optical field is

$$E_{\mathrm{TX}}^{(\mathrm{vsb})}(t) = \frac{1}{\sqrt{2}}\left[E_{\mathrm{TX}}^{(\mathrm{dsb})}(t) + j\,\mathcal{H}\left\{E_{\mathrm{TX}}^{(\mathrm{dsb})}(t)\right\}\right] \quad (26)$$

To a first approximation, the resulting signal is identical to the SSB-one. However, there is subtle, though significant, difference: the VSB signal is affected by clipping in the same way as DSB, since it has been generated with an ideal power-modulator.

2) Direct detection for VSB: Following the same steps performed in DSB and SSB, firstly ASE noise (10) is added, then the signal is filterered with an ideal OBPF, and finally is detected with an ideal photodiode. With the usual approximations, the received signal is:

$$z_0^{(\mathrm{vsb})}(t) \approx \frac{\bar{P}}{2}\,\mathcal{Q}\left[\frac{x(t)}{c'}\right] + n_{\mathrm{X,I}}(t)\sqrt{2\bar{P}\left\{1+\mathcal{Q}\left[\frac{x(t)}{c'}\right]\right\}} + \\ + \frac{\bar{P}}{2}\,\mathcal{H}^2\left\{\sqrt{\bar{P}\left\{1+\mathcal{Q}\left[\frac{x(t)}{c'}\right]\right\}}\right\} \quad (27)$$

Comparing this equation with DSB in (13), the first two terms (signal and ASE noise) are equal, except from scaling factors that do not affect the SNR. However, there is an additional term that is similar to SSBI in Single Side-Band (23), that induces a penalty at the receiver. Provided that this term is sufficiently compensated by proper DSP algorithms, the SNR is the same as DSB (16).

3) Non-linearity compensation: Due to the similarity with the SSB SSBI, the VSB SSBI term cancellation can be obtained applying a scheme as in Sec.II-C3

$$\hat{x}_{\mathrm{SSBI}}(t) = \gamma\,\mathcal{H}^2\left\{z_0^{(\mathrm{vsb})}(t) - \frac{1}{4}z_0^{2(\mathrm{vsb})}(t)\right\} \quad (28)$$

The terms inside Hilbert transform are the first two terms of the Taylor series expansion of the transmitted electric field (5). The effectiveness of this method is shown in Fig.5, where, similarly to Fig.4, there is an increase in performance, but smaller than that SSB. This is due to the joint effect of clipping, which cannot be compensated, and the approximation of the Taylor's series expansion. In Fig.3 VSB (dash-dot yellow line) is compared to SSB and DSB. The shape is similar to the other two methods: for high values of CSPR the performance gets closer to the asymptotic approximation, while for low values of CSPR the performance is limited by the joint effect of clipping and non-linear self-interference, which are not taken into account in the approximation (17). Due to these two effects, VSB has the worst performance compared to DSB and SSB.

E. Discussion

In Fig.6 the three methods are compared at different values of OSNR, and for each value of OSNR the CSPR is optimized and, when relevant, SSBI cancellation is applied with optimal parameters. In this figure, we also superimpose a horizontal line for the SNR value required to obtain a target BER=10^{-3}, which may be corrected to better than 10^{15} by a relatively

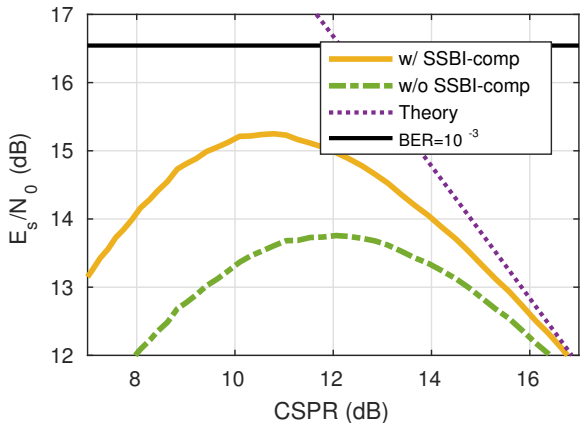

Fig. 5. SNR, geometrically averaged over all the subcarriers, of a 16-QAM DMT VSB-DMT signal, with (yellow solid line) and without (green dash-dot line) non-linear compensation. The results are compared to theory (16) (purple dotted line) and the required SNR to get BER=10^{-3}. The OSNR is 30 dB.

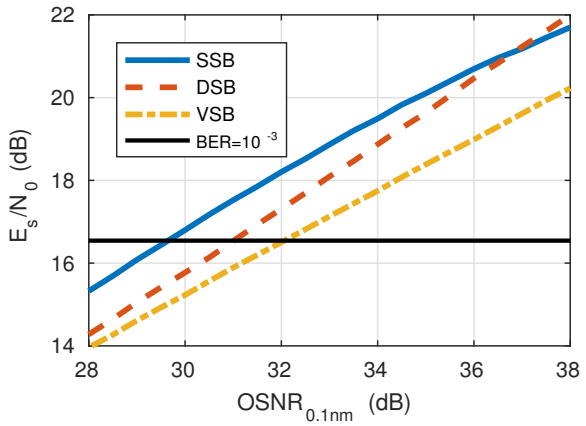

Fig. 6. Comparison of 16-QAM DMT SSB (blue solid line), DSB (red dashed line) and VSB (yellow dash-dot line) at their optimal CSPR for each OSNR. Results are compared with the required SNR to obtain BER=10^{-3}.

low overhead hard-decision FEC. This figure, together with the previous Fig.3 summarizes the most relevant result of this Section.

For small values of OSNR, DSB and VSB have similar performance, while SSB performs better than the other modulations by ~ 1 dB. At high values of OSNR, SSB floors due to SSBI estimation errors, while the performance of DSB and VSB linearly increase with the OSNR. For very high values of OSNR, DSB performs better compared to VSB due to the absence of self-interference terms.

From these back-to-back results we can conclude that, even without chromatic dispersion or DAC limitations, Single Side-Band has the highest performance for the OSNR ranges of interest, followed by DSB and VSB. In all cases, it is interesting to note that even in the very idealized channel conditions considered in this Section (*i.e.* in ASE noise only, without any type of optical or electrical bandwidth limitation) the required $\mathrm{OSNRs}_{@0.1nm}$ to obtain BER=10^{-3} are significant, and are higher than 30 dB in all cases. The main explanation for these values is due to the required CSPR, whose optimal values are of the order of more than 10 dB, meaning that the "useless"

optical CW carrier is 10 dB greater than the power of the modulated part of the spectrum. By slightly simplifying the analysis and for the DSB case only, we can say that more than 10 dB are "lost" due to the requirement of a "power-modulated" DMT signal, *i.e.* of the generation of an "always positive" transmitted electrical signal, which is a must for direct detection. Similar considerations hold also for SSB and VSB.

Considering system complexity, SSB has the highest transmitter cost/complexity, followed by VSB and DSB. Vestigial Side-Band in back-to-back has the worse performance and slightly higher transmitter cost compared to DSB, since it requires a sharp optical filter. As for the receiver complexity, both SSB and VSB require some non-linear self-interference compensation, which is not needed for DSB.

III. Impact of Chromatic Dispersion

In previous Section, the fundamental OSNR requirements were obtained for the three DMT variants in optical back to back. The present Section further develops the analysis, introducing some of the most relevant practical system limitations, starting with the effect of chromatic dispersion.

A. Effect on DSB

It is well known that for SSB-DMT and VSB-DMT, assuming a perfect sideband suppression, chromatic dispersion has no effect on the SNR [11] because it only generates a phase rotation on each subcarrier, which can be easily recovered through a standard one-tap DMT equalizer on each subcarrier.

The situation is completely different for DSB-DMT, as detailed in the following steps. The received electric field in presence of chromatic dispersion is:

$$E_{\mathrm{RX}}^{(\mathrm{dsb})}(t) = \left[E_{\mathrm{TX}}^{(\mathrm{dsb})}(t) \otimes h(t) + n_{\mathrm{X}}(t)\right] \hat{\mathbf{i}}_{\mathrm{X}} + n_{\mathrm{Y}}(t)\hat{\mathbf{i}}_{\mathrm{Y}} \quad (29)$$

where $\otimes$ denotes convolution, $h(t)$ is the chromatic dispersion impulse response and the transmitted electric field is defined in (1). As $h(t)$ is an all-pass filter, it has no effect on noise.

To analyze the problem, it is useful to expand $E_{\mathrm{TX}}^{(\mathrm{dsb})}(t)$ with a Taylor's series expansion (5) up to the 2nd order, obtaining

$$E_{\mathrm{TX}}^{(\mathrm{dsb})}(t) \otimes h(t) \approx \sqrt{\bar{P}}\left[1 + \frac{1}{2}\left(y(t) - \frac{y^2(t)}{4}\right) \otimes h(t)\right] \quad (30)$$

where $y(t)$ is defined in (6). By plugging (30) into (29), detecting it with an ideal photodiode, and applying the same approximations as (13), the signal becomes

$$z_0^{(\mathrm{dsb})}(t) \approx \bar{P}\left[\left(y(t) - \frac{1}{4}y^2(t)\right) \otimes \Re\{h(t)\} + \frac{1}{4}\left|\left(y(t) - \frac{1}{4}y^2(t)\right) \otimes h(t)\right|^2\right] + 2\sqrt{\bar{P}}n_{\mathrm{X,I}}(t) \quad (31)$$

Comparing this equation with the result without chromatic dispersion in (13), it can be seen that there are two main differences that can impact system performance.

The first is the well-known small-signal transfer function in a direct detection system [12], which is directly related to the $\Re\{h(t)\}$ filtering term in the previous equation, that give rise to the following transfer function:

$$H_{\mathrm{ss}}(\omega) = \cos\left(\omega^2 \frac{\beta_2}{2} d\right) \quad (32)$$

where $\omega = 2\pi(f - f_0)$, f_0 is the laser frequency, β_2 is the chromatic dispersion parameter and d is the propagation distance. For sufficiently high accumulated dispersion, this transfer function generates deep notches and consequently a system penalty for DSB-DMT.

A second and less known impact arises from the quadratic terms appearing in the second half of (31), which have some similarities to the SSBI terms in SSB (22) and VSB (27). The power of the quadratic terms, compared to the power of the signal, is inversely proportional to the CSPR, therefore for high CSPR they can be neglected, leading to the power-power transfer function with the small-signal approximation (32).

To check if this approximation applies to the system under study for the values of interest of CSPR (*i.e.* those discussed in previous Section), a numerical simulation of DSB-DMT signal transmission has been set up. A DSB-DMT signal is power modulated with 10 dB of CSPR. It is then transmitted over 80 km of linear Standard Single-Mode optical Fiber (SSMF) ($D = 16.7$ ps/(nm km), $f_0 = 193.4$ THz), amplified with a noiseless amplifier and detected with an ideal photodiode.

The histograms of the transmitted (*a*) and received electrical signals (*b*) are shown in Fig.7. As expected, the transmit signal is almost perfectly Gaussian (as it has to be for a DMT signal with a high number of subcarriers, 2048 in our simulations), while the received signal is clearly not Gaussian. But if the system had been linear, the received signal would have been Gaussian. This observation clearly proves that there is a significant nonlinear effect, which is due to the quadratic terms in (31), which evidently cannot be neglected for the CSPR values of interest. Quite unexpectedly, it was found that this nonlinearity creates a significant additional penalty in DSB-DMT in presence of strong accumulated dispersion.

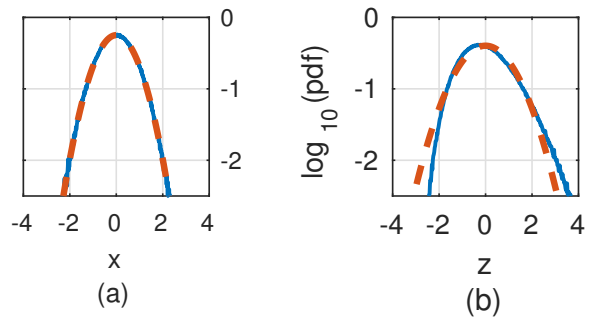

Fig. 7. Histograms in logarithmic scale of a DSB DMT signal (solid blue line) at the transmitter, immediately before power modulation (*a*), and immediately after the photodiode (*b*) (DC is removed). The signals have been scaled to set their variance to 1. ASE noise is not present, the CSPR is 10 dB, propagation distance is 80 km of SSMF. Red dashed line is a Gaussian fit of the two histograms.

B. A predistortion proposal for DSB-DMT

The effect of the quadratic terms in DSB with chromatic dispersion can be reduced by means of transmitter predistor-

tion. By changing (1) into

$$\tilde{E}_{\mathrm{TX}}^{(\mathrm{dsb})}(t) = \sqrt{\bar{P}\left\{1 + 2\,\mathcal{Q}\left[\frac{x(t)}{2c'}\right] + \mathcal{Q}^2\left[\frac{x(t)}{2c'}\right]\right\}} \tag{33}$$

the transmitted electric field simplifies to

$$\tilde{E}_{\mathrm{TX}}^{(\mathrm{dsb})}(t) = \sqrt{\bar{P}}\left\{1 + \mathcal{Q}\left[\frac{x(t)}{2c'}\right]\right\} \tag{34}$$

approximating a field-modulated signal, similar to SSB (19). This is achieved by adding a quadratic term $\mathcal{Q}^2\left[x(t)/2c'\right]$ to the DAC output, before power modulation.

Following the same steps performed in Section II-B, the signal after photodetection becomes

$$\tilde{z}_0^{(\mathrm{dsb})}(t) \approx 2\bar{P}\,\mathcal{Q}\left[\frac{x(t)}{2c'}\right] \otimes \Re\{h(t)\} + \\ + \bar{P}\left|\mathcal{Q}\left[\frac{x(t)}{2c'}\right] \otimes h(t)\right|^2 + 2\sqrt{\bar{P}} n_{\mathrm{X,I}}(t) \tag{35}$$

Compared to (31), there is only one quadratic term left, which is very similar to SSBI for SSB (23). Therefore, it can be estimated using a method similar to (25) but even simpler, since there is no need to evaluate a Hilbert transform. By combining pre-distortion and receiver compensation, the channel can be completely linearized, and the only impairment of chromatic dispersion is the small-signal transfer function (32), which can be now handled with one of the well-known bit and power loading algorithms, such as the Levin-Campello algorithm used in the following Subsection.

C. Simulation setup

In order to evaluate the impact of chromatic dispersion for the three methods, as well as the effectiveness of the newly proposed non-linear pre- and post- compensation for DSB, a numerical DMT simulation has been set up, similar to the simulation used for the results in Section II but without neglecting any linear or nonlinear terms.

The FFT size is 1024, and the DAC sampling rate is $R_{\mathrm{s}} = 64$ Gs/s. The channel introduces chromatic dispersion in addition to ASE noise, assuming a linear SSMF with $D = 16.7$ ps/(nm km); the central frequency of the signal is $f_0 = 193.4$ THz ($\lambda_0 = 1550$ nm). The DAC and ADC are ideal (*i.e.* no filtering and no quantization), as well as the optical modulators. Before the photodiode, an OBPF is inserted to filter out-of-band noise. As described in Section II, the bandwidth of these filters is $R_{\mathrm{s}}/2$ for SSB and VSB, and R_{s} for DSB.

The choice of the optical filters (both at transmitter and receiver) for VSB is crucial, since it represents a trade-off between filter complexity and sideband suppression. An ideal rectangular filter, or a 2nd-order SuperGaussian filter with a 3-dB bandwidth of 35-GHz are assumed. The SuperGaussian filter is a standard shape for 50-GHz grid Wavelength Division Multiplexing (WDM) filters. On the other end, the shape of the receiver optical filter for SSB and VSB is not crucial, since its purpose is the suppression of out-of-band ASE noise, therefore we used ideal (*i.e.* rectangular) filters.

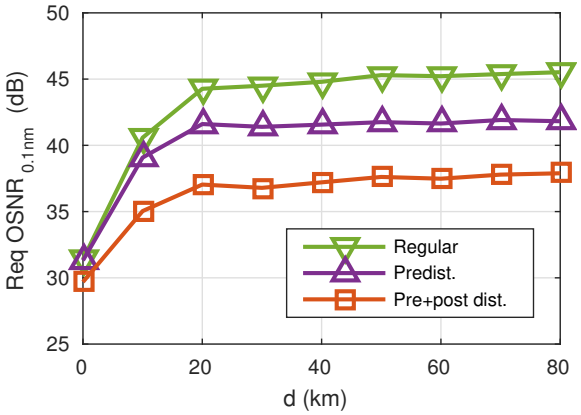

Fig. 8. Required OSNR (over 0.1 nm) to obtain BER $= 10^{-3}$ for DSB-DMT as a function of distance of SSMF. Regular DSB (1) (green downward-pointing triangles), DSB with only predistortion (33) (purple upward-pointing triangles), DSB with predistortion and receiver non-linearity compensation (red squares). CSPR is optimized for every point.

All three DMT variants adopted bit and power loading. To this end, every simulation starts with a calibration phase, where the electrical SNR is measured on all subcarriers using random 16-QAM training symbols. Then the Levin-Campello bit and power loading algorithm [13], [14] (in the so called margin adaptive version, *i.e.* for a total fixed bit rate) selects the most suitable gain and modulation format for each subcarrier, spanning between BPSK and 128-QAM, in order to achieve a gross bit-rate $R_{\mathrm{b}} = 120$ Gb/s. After that, a random signal with this bit and power profile is generated and sent over the same channel, and the average BER is computed. The cyclic prefix length is 44 samples. This length has been chosen to compensate for the pulse spreading caused by chromatic dispersion.

D. Simulation results

1) DSB non-linearity compensation: In order to test the effectiveness of the proposed DSB quadratic-terms compensation method, the required OSNR (over an optical bandwidth of 0.1 nm) to achieve an average BER of 10^{-3} was calculated for a DSB-DMT signal with different amounts of chromatic dispersion.

The results are shown in Fig.8. At 80 km, the required OSNR for "regular" DSB is 45.5 dB, which represents a penalty of 14.1 dB compared to back-to-back. Predistortion reduces the required OSNR by 3.7 dB, and predistortion followed by the compensation of the quadratic term at the receiver will reduce it by another 4.4 dB. It is also interesting to see that the OSNR penalty due to dispersion grows quickly in the first 20 km in the considered scenario (*i.e.* $R_{\mathrm{b}} = 120$ Gb/s in the C band of SSMF fibers), then it reaches an almost horizontal plateau where penalty grows only marginally. After investigating in detail this effect, it was found a simple explanation. For increasing fiber distance, the penalty grows quickly when the first notch in the transfer function $H_{\mathrm{ss}}(f)$ in (32) enters in the DSB-DMT band (*i.e.* it goes below $R_s/2$) then it "stabilizes" with a marginal increment in penalty above 20 km. This is mainly due to the change of shape of $H_{\mathrm{ss}}(f)$,

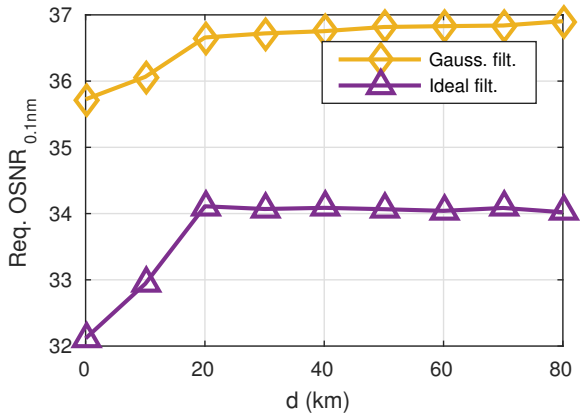

Fig. 9. Required OSNR (over 0.1 nm) to obtain BER $= 10^{-3}$ for VSB-DMT as a function of distance of SSMF. Ideal (*i.e.* rectangular) optical filter at transmitter (purple triangles), 2nd-order SuperGaussian optical filter with 3-dB bandwidth of 35-GHz (yellow diamonds).

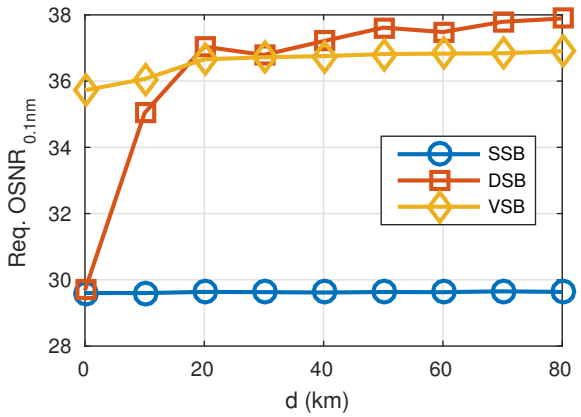

Fig. 10. Required OSNR (over 0.1 nm) to obtain BER $= 10^{-3}$ for SSB (blue circles), DSB with predistortion and receiver compensation (red squares) and VSB with a SuperGaussian optical filter (yellow diamonds).

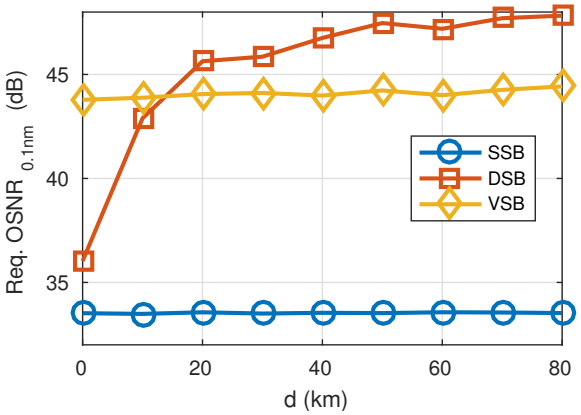

Fig. 11. Required OSNR (over 0.1 nm) to obtain BER $= 10^{-3}$ for SSB (blue circles), DSB (red squares) and VSB (yellow diamonds), with a realistic DAC and ADC. The DSP is the same as Fig.10.

that makes less accurate the approximation that the channel frequency response is flat inside each subcarrier [8], leading to an additional penalty.

We also simulate a bit and power loading algorithm assuming that the electrical-to-electrical channel is completely linear and characterized by the small-signal transfer function $H_{\rm ss}(f)$. The resulting penalty curve almost completely superimposes with the bottom curve in Fig.8, demonstrating that the newly proposed pre- and post- compensation is able to completely "linearize" the chromatic dispersion direct detection channel.

2) VSB optical filter: As stated previously, the optical filter for VSB is a crucial component, since it represents a trade-off between complexity of the filter and sideband suppression. A non-perfect sideband suppression will introduce penalties due to chromatic dispersion, since the remaining sideband will interfere with the other sideband in a way similar to DSB due to the $H_{\rm ss}(f)$ electrical to electrical transfer function effect.

In Fig.9 it is shown the required OSNR for a VSB system using either ideal (*i.e.* rectangular) optical filters and two 2nd-order SuperGaussian optical filters, with 3-dB bandwidth of 35-GHz and central frequency shifted by 16-GHz with respect to the laser frequency; this frequency shift has been optimized. The filters are put both at the transmitter (to suppress one sideband) and at the receiver (to remove out-of-band noise). At 80 km, the OSNR penalty is 2.88 dB.

3) Overall comparison SSB-DSB-VSB: The results obtained in Fig.8 and 9 are collected in Fig.10, where the three methods are compared with distance. These graphs were obtained at optimal CSPR which for instance at 80 km is 10.5 dB for SSB, 13 dB for DSB and 16 dB for VSB. SSB has no penalty with distance (at least assuming an ideal DAC and modulator, as it was done so far in this paper), since the sideband is completely suppressed and chromatic dispersion has almost no effect. SSB-DMT thus requires an OSNR of 29.6 dB for all considered distances. As for DSB and VSB, the difference between the two methods at 80 km is very small (1 dB), since the effect of chromatic dispersion for DSB is partially compensated by bit loading, which has no penalty since, again, it is assumed an ideal DAC without quantization. It is expected that quantization will have a higher impact on DSB than the other modulation formats, increasing its required OSNR, as it is analyzed in the following Section IV.

IV. Quantization and Bandwidth Limitations

To investigate the effect of DAC and ADC resolution, we modeled the DAC as a 5-bit quantizer and the ADC with 8 bits, in order to have overall about 5 effective quantization bits. These values have been selected according to the typical resolution and bandwidths of current high-speed ADCs and DACs, which today are usually specified at about 5.5 Effective Number of Bits (ENoB). Low-pass construction and anti-aliasing filters were also inserted in our realistic simulations while, for simplicity, electronic noise was not modeled, since it is expected to be negligible in an optically amplified system as the one we are considering. The DAC low-pass filter is a single-pole filter with 3-dB frequency at 10.3 GHz followed by an ideal *sinc* with first zero at $R_{\rm s}$. This model has been chosen to be similar to the frequency response of a reference DAC running at $R_{\rm s} = 64$ Gs/s.

The effect of quantization on the three methods is shown in Fig.11. The DSP is the same adopted for Fig.10, with the only

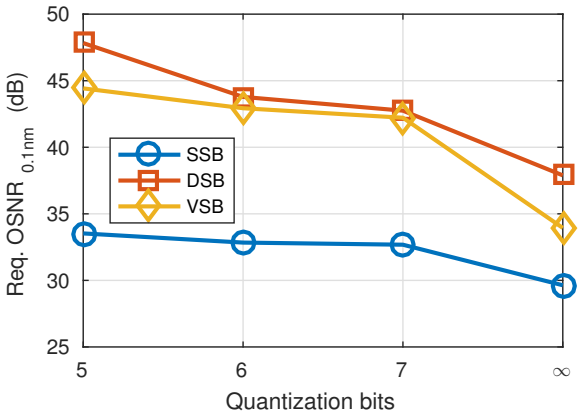

Fig. 12. Required OSNR (over 0.1 nm) to obtain BER $= 10^{-3}$ for SSB (blue circles), DSB (red squares) and VSB (yellow diamonds), with different number of DAC quantization bits, at 80 km SSMF.

difference of DAC and ADC. At 80 km, SSB has a penalty of 3.9 dB compared to the ideal DAC case, while VSB and DSB have a higher penalty (7.5 and 10 dB, respectively). An intuitive explanation of the higher penalty for DSB compared to SSB can be easily given: due to the frequency response that DSB sees when chromatic dispersion is relevant (such as at 80 km), the margin-adaptive bit and power loading algorithm forces higher cardinality QAM constellations on some of the DMT subcarriers. In particular, for the cases of interest at about 80 km, the DSB bit loading requires constellation up to 128-QAM, and these constellations are much more sensitive to quantization problems compared to the 16-QAM constellation that is requested on most of the subcarriers for the SSB case (which sees a relatively flat electrical-to-electrical transfer function even for strong dispersion). Enforcing the quantization requirements to higher number of bits, the penalty at 80 km decreases as shown in Fig.12, where the required OSNR at 80 km is plotted for different quantization bits (the last point to the right end side of the figure is for a situation without any quantization).

V. Conclusion

We addressed in this paper three different DMT variants in the scenario of medium reach (up to 80 km over SMF fibers used in the C-band) optically pre-amplified and dispersion uncompensated systems, finding that SSB seems the only DMT option that is doable in terms of required OSNR. As an example, we found that under realistic conditions shown in Sec.IV, a 100 Gbps (net) SSB-DMT solutions at 80 km and BER=10^{-3} would require approximately 34 dB $\text{OSNR}_{0.1\text{nm}}$ (see Fig.12) for 5 quantization bits. For an optical preamplifier with a 5 dB noise figure, a 34 dB received $\text{OSNR}_{0.1\text{nm}}$ would translate into a -19 dBm received power requirement so that, for instance, at 0.2 dB/km optical fiber attenuation this would translate into a -3 dBm required transmit power per wavelength, which seems promising even when considering a realistic system margin. Just as an example, considering a 3 dB system margin, the resulting 0 dBm transmitted power requirement should not be critical in terms of nonlinear Kerr impairments in the fiber, considering also the relatively short transmission distances involved.

We also would like to mention that the SSB-DMT optical spectral occupation is compliant with a 50 GHz DWDM spacing, which at 100 Gbps per λ provides an overall net spectral efficiency of 2 bit/s/Hz in direct detection.

Acknowledgment

The authors would like to thank Cisco Photonics for partially supporting this research activity.

References

[1] S. Randel, D. Pilori, S. Chandrasekhar, G. Raybon, and P. Winzer, "100-Gb/s discrete-multitone transmission over 80-km SSMF using single-sideband modulation with novel interference-cancellation scheme," in *Optical Communication (ECOC), 2015 European Conference on*. IEEE, 2015, pp. 1–3.

[2] A. Dochhan, H. Griesser, N. Eiselt, M. H. Eiselt, and J. P. Elbers, "Solutions for 80 km DWDM systems," *Journal of Lightwave Technology*, vol. 34, no. 2, pp. 491–499, 2016.

[3] M. Sharif, J. K. Perin, and J. M. Kahn, "Modulation schemes for single-laser 100 gb/s links: Single-carrier," *Journal of Lightwave Technology*, vol. 33, no. 20, pp. 4268–4277, 2015.

[4] J. K. Perin, M. Sharif, and J. M. Kahn, "Modulation schemes for single-laser 100 gb/s links: Multicarrier," *Journal of Lightwave Technology*, vol. 33, no. 24, pp. 5122–5132, 2015.

[5] L. Zhang, T. Zuo, Y. Mao, Q. Zhang, E. Zhou, G. Liu, and X. Xu, "Beyond 100-Gb/s transmission over 80-km SMF using direct-detection SSB-DMT at C-band," *Journal of Lightwave Technology*, vol. 34, no. 2, pp. 723–729, 2016.

[6] L. Nadal, M. S. Moreolo, J. M. Fàbrega, A. Dochhan, H. Grießer, M. Eiselt, and J.-P. Elbers, "DMT modulation with adaptive loading for high bit rate transmission over directly detected optical channels," *Journal of Lightwave Technology*, vol. 32, no. 21, pp. 3541–3551, 2014.

[7] W.-R. Peng, X. Wu, K.-M. Feng, V. R. Arbab, B. Shamee, J.-Y. Yang, L. C. Christen, A. E. Willner, and S. Chi, "Spectrally efficient direct-detected OFDM transmission employing an iterative estimation and cancellation technique," *Optics Express*, vol. 17, no. 11, pp. 9099–9111, 2009.

[8] J. M. Cioffi, "Chapter 4 – multi-channel modulation," in *Lecture notes for advanced digital communications*. Stanford University, 2001.

[9] Z. Li, M. S. Erkılınç, R. Bouziane, B. C. Thomsen, P. Bayvel, and R. I. Killey, "Simplified DSP-based signal–signal beat interference mitigation technique for direct detection OFDM," *Journal of Lightwave Technology*, vol. 34, no. 3, pp. 866–872, 2016.

[10] C. Ju, N. Liu, and X. Chen, "Comparison of iteration interference cancellation and symbol predistortion algorithm for direct detection orthogonal frequency division multiplexing passive optical network," *Optical Engineering*, vol. 54, no. 8, pp. 086 104–086 104, 2015.

[11] K. Yonenaga and N. Takachio, "A fiber chromatic dispersion compensation technique with an optical SSB transmission in optical homodyne detection systems," *Photonics Technology Letters, IEEE*, vol. 5, no. 8, pp. 949–951, 1993.

[12] J. Wang and K. Petermann, "Small signal analysis for dispersive optical fiber communication systems," *Journal of Lightwave Technology*, vol. 10, no. 1, pp. 96–100, 1992.

[13] H. E. Levin, "A complete and optimal data allocation method for practical discrete multitone systems," in *Global Telecommunications Conference, 2001. GLOBECOM'01. IEEE*, vol. 1. IEEE, 2001, pp. 369–374.

[14] J. Campello, "Practical bit loading for DMT," in *Communications, 1999. ICC'99. 1999 IEEE International Conference on*, vol. 2. IEEE, 1999, pp. 801–805.

Dario Pilori received his B.Sc. and M.Sc. degrees in Telecommunications Engineering from Politecnico di Milano (Italy) in, respectively, 2012 and 2015. He spent one year, between 2013 and 2014, in Alcatel-Lucent (now Nokia) Bell Laboratories, Holmdel NJ (U.S.A.) as an intern, working on Digital Signal Processing for high-speed optical communications. From 2015

he is a Ph.D. candidate at Politecnico di Torino (Italy). His current research interest are in DMT-based short and medium reach optical communication systems.

Chris Fludger is a Principal Engineer at Cisco Optical (formally CoreOptics) in Germany where he designs optical transceivers and linecards, incorporating advanced signal processing and modulation techniques. He formally worked on DSP and Raman amplification at Nortel Networks Research Laboratories, Harlow, U.K. He received the M.Eng. degree with distinction, and the Ph.D. degree in electronic engineering from Cambridge University, UK. Dr Fludger is a Chartered Engineer and member of the Institute of Engineering and Technology.

Roberto Gaudino Ph.D., is currently Associate Professor at Politecnico di Torino, Italy. His main research interests are in the long haul DWDM systems, fiber non-linearity, modelling of optical communication systems and in the experimental implementation of optical networks, with specific focus on access networks. In particular, in the last five years, he focused his activity on short-reach optical links using plastic optical fibers (POF) and on next-generation passive optical access networks (NG-PON2). Currently, he is working on ultra high capacity systems for medium reach links. Previously, he worked extensively on fiber modelling, optical modulation formats (such as duo-binary, polarization or phase modulation), coherent optical detection, and on the experimental demonstration of packet switched optical networks. Prof. Gaudino spent one year in 1997 at the Georgia Institute of Technology, Atlanta, as a visiting researcher, where he worked in the realization of the MOSAIC optical network test-bed. From 1998, he was with the team that coordinated the development of the commercial optical system simulation software OptSim (Artis Software Corp., then acquired by RSoft Design and now by Synopsys). He has consulted for several companies and he is author or co-author of approximately 200 papers in the field of Optical Fiber Transmission and Optical Networks. He has been the coordinator of the EU FP6-IST STREP project POF-ALL, “POF-PLUS” and currently is the scientific coordinator of the EU FP7-ICT STREP project FABULOUS, all three projects in the area of optical access.